UKACC International Conference on Control 2012
Cardiff, UK, 3-5 September 2012

Control Allocation for Fault Tolerant Control of a VTOL Octorotor

Aryeh Marks
Department of
Aerospace Engineering
Cranfield University
Bedfordshire, U.K.
MK43 0AL
Email:a.marks@cranfield.ac.uk

James F Whidborne
Department of
Aerospace Engineering
Cranfield University
Bedfordshire, U.K.
MK43 0AL
Email:j.f.whidborne@cranfield.ac.uk

Ikuo Yamamoto
Graduate School of
Environmental Engineering
The University of Kitakyushu
Fukuoka
Japan
Email:yamamoto@env.kitakyu-u.ac.jp

***Abstract*—For the fault tolerant control of an eight-rotor VTOL Unmanned Air Vehicle (UAV), a control allocation scheme is proposed. The eight-rotor configuration provides actuator redundancy to ensure safe operation under rotor/motor failures. A PD controller is used to generate total thrust and moment demands. A cascade inverse method of control allocation is proposed to allocate the controller commands to the actuators whilst ensuring that actuator saturation does not occur. If the vehicle is subjected to rotor failures, the scheme re-allocates the commands to maintain the vehicle stability and performance. Until actuator saturation occurs the response of the vehicle is the same when operating with all motors or fewer. The response of the vehicle to several combinations of complete actuator failures is investigated by simulation and it is shown that the proposed method is able to maintain control after failure of up to four actuators. The controller is invarient and the vehicle response to commands is identical until motor saturation occurs.**

***Index Terms*—Control Allocation, VTOL UAV, Octorotor, Fault Tolerance**

I. Introduction

Unmanned Air Vehicles (UAVs) capable of Vertical Take-off and Landing (VTOL) operations can provide many advantages over conventional manned aircraft and UAVs which are not capable of such flight. They give mission flexibility in that a runway is not needed for launch and recovery, give a stable platform for capturing images due to their hover capability, are capable of high agility maneuvers such as vertical drops [1] and allow for operations in harsh and hostile environments since they do not put a human operator at risk. One major drawback with using conventional quadrotor vehicles such as OS4 [2], STARMAC [3], Qball-X4 [4] and tri-rotor vehicles [5] is that there is no effector redundancy. If a rotor fails completely then control is lost and the vehicle may crash. This is an unacceptable scenario when operating over populated urban areas.

It is fairly straightforward to demonstrate that complete loss of a rotor for a quadrotor results in a vehicle that is not fully controllable. However, with a partial failure in one rotor, a quadrotor is still controllable. Fault detection and recovery schemes have been investigated for a 50% thrust reduction in one rotor by [6] and, using a sliding mode method, by [7]. Other methods for partial failures can be found in [4], [8]. Fault tolerant control for a quadrotor subject to sensor failures has been investigated by [9] and by [10]. Even though a total loss of a rotor results in an uncontrollable vehicle, it has been shown that partial control can be maintained [11] with a loss of yaw control.

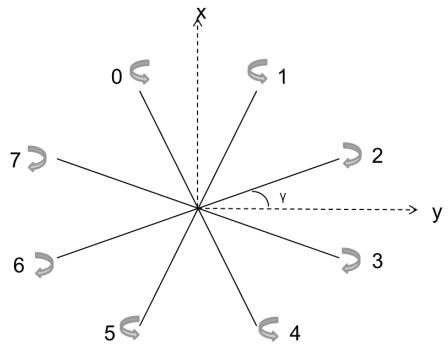

Fig. 1. Octorotor Schematic Layout

TABLE I
Vehicle Parameters

Thrust factor, b	3.13×10^{-5}
Drag factor, d	7.5×10^{-7}
Inertia I_x, I_y	7.5×10^{-3}kg m^2
Inertia I_z	1.3×10^{-2}kg m^2
Rotor Inertia, J	6×10^{-5}kg m^2
Length of arm, l	0.4m
Vehicle mass, m	1.2kg
γ	22.5°

The octorotor has been proposed as a solution to the problem of safe operation of quadrotor-like UAVs [12], [13]. A schematic of the vehicle is shown in Figure 1 with parameters shown in table I. With eight independently controllable rotors the vehicle has in-built hardware redundancy. Combinations of various rotor thrusts will provide moments causing the vehicle to roll around the x axis and pitch around the y axis. Yaw control is achieved by varying the thrust from

the clockwise and counter-clockwise rotors whilst keeping a constant overall thrust value. This generates an imbalance in the gyroscopic drag causing the vehicle to yaw around the z axis. Furthermore, if the thrust of any single rotor is changed then it will generate a rolling, pitching and yawing moment. This is a property that can be exploited when fewer than eight rotors are utilized.

It is possible to use various combinations of rotors to generate moments across the body. The allocation and mixing of the thrust demands to achieve a desired objective is the control allocation problem. Various methods for linear control allocation have been proposed including explicit ganging [14], rule based systems [15, pp. 89-106] which have switches in the control laws depending on the failure scenario, daisy chaining [16] which divides the actuators into sets that can perform the same task and are then ranked according to preference for usage and effectiveness until the requirements are met or the maximum performance from the set is reached. On-line optimization methods have been proposed, see [17] for a review. The most common approach uses constrained quadratic programming (e.g. [18], [19], [20], [21], [22]) and this results in efficient solutions. A Redistributed Pseudo Inverse (RPI) method [21] is used in this paper. This method can increase the possibility of reaching an optimal solution to an inverse problem and allows for actuator saturation to be considered. A comparison of control allocation methods with control effectiveness uncertainties [23] has shown that the RPI method leads to low errors and high performance.

This paper proposes the use of controller reallocation as a means of obtaining fault tolerant control of the octorotor vehicle subject to failures in one or more rotors. Stability and performance of the vehicle is maintained by means of an RPI control reallocation scheme. The performance of the vehicle subject to multiple rotor failures is shown by simulation. The authors believe this is the first work to show full controllability of all states for a VTOL UAV after rotor failures.

In Section II the dynamics of the octorotor are presented. The essential dynamics are well known [24], [25], [26] but this work focusses on the application to a vehicle with eight rotors rather than the four found in other work [2], [3]. The controller tasked with stabilizing the body angles and global altitude is developed in Section III. A description of rotor saturation and control allocation via the RPI method is given in Section IV. Section V shows results from numerical simulations showing how the control re-allocation can control the vehicle with hardware failures.

II. Octorotor Dynamics

A. Dynamics Model

The dynamics of small VTOL UAVs are well developed. Here, the Newton-Euler approach is used [24], [25], [26] with the following assumptions:

- the structure is rigid and symmetric,
- the propellers are rigid,
- the thrust and the drag are proportional to the square of the speed of the rotor,
- ground effect is neglected,
- the inertia matrix is diagonal,
- the rotor Coriolis force and wind forces are not included,
- and the motor dynamics are ignored.

The state variables used in this analysis are:

$$X = [U\ V\ W\ P\ Q\ R\ x\ y\ z\ \phi\ \theta\ \psi]^T \tag{1}$$

where U, V, W are the body-centric velocities of the vehicle, P, Q, R are the rotation rates, x, y, z describe the global position of the vehicle in the inertial frame and ϕ, θ, ψ are the Euler angles. Consider a body-fixed frame with the x,y, and z axes originating at the center of mass of the vehicle. An inertial frame is fixed to the Earth and has axes in the conventional North-East-Down arrangement. The orthogonal rotation matrix S_b converts from a body-fixed coordinate system to the Earth-fixed coordinate system with the assumptions that

- the Earth is flat and stationary and
- the center of gravity lies at the origin of the body axis reference frame

and is given by

$$S_b = \begin{bmatrix} c\theta c\psi & c\theta s\psi & -s\theta \\ s\phi s\theta c\psi - c\phi s\psi & c\phi c\psi + s\phi s\theta s\psi & c\theta s\phi \\ c\phi s\theta c\psi + s\phi s\psi & c\phi s\theta s\psi - s\phi c\psi & c\theta c\phi \end{bmatrix} \tag{2}$$

where $s\phi = \sin\phi$, $c\phi = \cos\phi$ etc. This notation is used throughout the paper.

The total forces and moments in the body axis are given by

$$F_{net} = \frac{d}{dt}[m\mathbf{V}] + \omega' \times [m\mathbf{V}] \tag{3}$$

$$M_{net} = \frac{d}{dt}[I\omega'] + \omega' \times [I\omega'] \tag{4}$$

where $\mathbf{V}$ is the vector of linear velocities, ω' is the vector of angular velocities, I is the inertia matrix and m is the mass of the vehicle. The gravitational force F_g is

$$F_g = m\ S_b \begin{bmatrix} 0 \\ 0 \\ g \end{bmatrix} = mg \begin{bmatrix} -s\theta \\ c\theta s\phi \\ c\theta c\phi \end{bmatrix} \tag{5}$$

where g is the acceleration due to gravity. The total force F_{net} is the force of gravity and the forces generated through the rotors, F_p,

$$F_{net} = F_g + F_p, \tag{6}$$

which from (3) gives

$$\begin{bmatrix} \dot{U} \\ \dot{V} \\ \dot{W} \end{bmatrix} = \frac{1}{m} \begin{bmatrix} F_{px} \\ F_{py} \\ F_{pz} \end{bmatrix} + g \begin{bmatrix} -s\theta \\ c\theta s\phi \\ c\theta c\phi \end{bmatrix} - \begin{bmatrix} QW - RV \\ RU - PW \\ PV - QU \end{bmatrix} \tag{7}$$

From (4), the total moments M_{net} acting on the vehicle are

$$M_{net} = \begin{bmatrix} M_x \\ M_y \\ M_z \end{bmatrix} = \begin{bmatrix} I_x & 0 & 0 \\ 0 & I_y & 0 \\ 0 & 0 & I_z \end{bmatrix} \begin{bmatrix} \dot{P} \\ \dot{Q} \\ \dot{R} \end{bmatrix} + \begin{bmatrix} P \\ Q \\ R \end{bmatrix} \times \begin{bmatrix} I_x & 0 & 0 \\ 0 & I_y & 0 \\ 0 & 0 & I_z \end{bmatrix} \begin{bmatrix} P \\ Q \\ R \end{bmatrix} \tag{8}$$

Rearranging in terms of the state variable derivatives gives

$$\begin{bmatrix}\dot{P}\\ \dot{Q}\\ \dot{R}\end{bmatrix} = \begin{bmatrix}M_x/I_x\\ M_y/I_y\\ M_z/I_z\end{bmatrix} - \begin{bmatrix}((I_z-I_y)/(I_x))\,QR\\ ((I_x-I_z)/(I_y))\,RP\\ ((I_y-I_x)/(I_z))\,PQ\end{bmatrix} \tag{9}$$

The rotation matrix, S_b, from (2) is used to express the movement of the vehicle in the global axes once the body-centric velocities are known:

$$\begin{aligned}\begin{bmatrix}\dot{x}\\ \dot{y}\\ \dot{z}\end{bmatrix} &= S_b^T \begin{bmatrix}U\\ V\\ W\end{bmatrix}\\ &= \begin{bmatrix}c\psi c\theta & c\psi s\theta s\phi - s\psi c\phi & c\psi s\theta c\phi + s\psi s\phi\\ s\psi c\theta & s\psi s\theta s\phi + c\psi c\phi & s\psi s\theta c\phi - c\psi s\phi\\ -s\theta & c\theta s\phi & c\theta c\phi\end{bmatrix}\begin{bmatrix}U\\ V\\ W\end{bmatrix}\end{aligned} \tag{10}$$

The flight path is found by integrating (10). It contains the body-centric Euler angles and these are related to the global body angles through

$$\begin{bmatrix}P\\ Q\\ R\end{bmatrix} = \begin{bmatrix}1 & 0 & -s\theta\\ 0 & c\phi & s\phi c\theta\\ 0 & -s\phi & c\theta c\phi\end{bmatrix}\begin{bmatrix}\dot{\phi}\\ \dot{\theta}\\ \dot{\psi}\end{bmatrix} = S_e^{-1}\begin{bmatrix}\dot{\phi}\\ \dot{\theta}\\ \dot{\psi}\end{bmatrix}$$

giving

$$\begin{bmatrix}\dot{\phi}\\ \dot{\theta}\\ \dot{\psi}\end{bmatrix} = S_e \begin{bmatrix}P\\ Q\\ R\end{bmatrix} \tag{11}$$

where

$$S_e = \begin{bmatrix}1 & t\theta s\phi & t\theta c\phi\\ 0 & c\phi & -s\phi\\ 0 & s\phi/c\theta & c\phi/c\theta\end{bmatrix} \tag{12}$$

B. State Space Model

The general state space model $\dot{X} = f(X,\Gamma)$ is obtained from (7), (9), (10), (11) and (17) with state variables given by (1) and control given by

$$\Gamma = \begin{bmatrix}F_{pz}\\ M_p\end{bmatrix} \tag{13}$$

where $M_p = M_{net}$. This gives the state equation

$$\frac{d}{dt}\begin{bmatrix}U\\ V\\ W\\ P\\ Q\\ R\\ x\\ y\\ z\\ \phi\\ \theta\\ \psi\end{bmatrix} = \begin{bmatrix}-g\ s\theta - (QW - RV)\\ g\ c\theta s\phi - (RU - PW)\\ (-c\theta c\phi F_{pz}/m) + g\ c\theta c\phi - (PV - QU)\\ (M_x/I_x) - ((I_z - I_y)/I_x)\,QR\\ (M_y/I_y) - ((I_x - I_z)/I_y)\,RP\\ (M_z/I_z) - ((I_y - I_x)/I_z)\,PQ\\ (c\psi c\theta)U + (c\psi s\theta s\phi - s\psi c\phi)V + (c\psi s\theta c\phi + s\psi s\phi)W\\ (s\psi c\theta)U + (s\psi s\theta s\phi + c\psi c\phi)V + (s\psi s\theta c\phi - c\psi s\phi)W\\ -s\theta U + (c\theta s\phi)V + (c\theta c\phi)W\\ P + (t\theta s\phi)Q + (t\theta c\phi)R\\ c\phi Q - s\phi R\\ (s\phi/c\psi)Q + (c\phi/c\theta)\,R\end{bmatrix} \tag{14}$$

C. Actuator Model

The total force provided by the rotors in the body frame is

$$F_{pz} = \sum_{i=0}^{7} b\ \Omega_i^2 \tag{15}$$

where b is the term relating the rotor thrust to the squared rotor speed Ω_i^2. The rotor axes are mounted vertically on the vehicle so

$$F_{px} = F_{py} = 0 \tag{16}$$

The moments, M_x, M_y, M_z, are generated by the differences in the thrusts of the eight rotors. The relationship between the control Γ and the rotor speeds is given by

$$\Gamma = \Lambda\Sigma \tag{17}$$

where Σ is the vector containing the squared rotor speeds

$$\Sigma = \begin{bmatrix}\Omega_0^2 & \Omega_1^2 & \Omega_2^2 & \Omega_3^2 & \Omega_4^2 & \Omega_5^2 & \Omega_6^2 & \Omega_7^2\end{bmatrix}^T, \tag{18}$$

and Λ is the control allocation matrix

$$\Lambda = \begin{bmatrix}b & b & b & b & b & b & b & b\\ b_s & -b_s & -b_c & -b_c & -b_s & b_s & b_c & b_c\\ -b_c & -b_c & -b_s & b_s & b_c & b_c & b_s & -b_s\\ d & d & -d & -d & d & d & -d & -d\end{bmatrix}, \tag{19}$$

where $b_s = bl\sin\gamma$, $b_c = bl\cos\gamma$ and where γ denotes the angle between the arms of the vehicle and the major axis lines as shown in Figure 1, l denotes the arm length from the center of the vehicle to the rotor axis, the factor b relates the squared rotor speed Ω_i^2 to the thrust and the drag factor d relates the gyroscopic drag to the squared rotor speed.

III. Controller

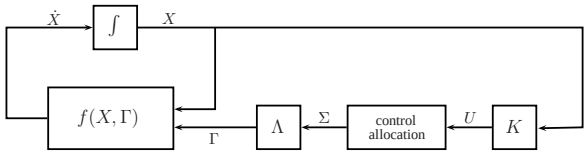

Fig. 2. System Block Diagram

Figure 2 shows the block diagram of the system which is assumed to provide perfect control allocation, that is $\Gamma = U$. The number of rotors and the allocation of the control demands, Σ, are not considered in the control block where the output, U, is simply a moment demand. This means that any maneuvers are completed with the same performance regardless to the number of functional rotors. The operator should not notice any performance change with rotor/motor failures unless all actuators are saturated.

Even though the vehicle has eight physical actuators the system is under actuated in that the actuators can only directly affect four of the six degrees of freedom. For this reason only four control demands can be performed. The control Γ (17) contains the total thrust and three moment demands and corresponds to commands U_i, $i = 1, 2, 3, 4$.

To design the controller, several further assumptions are made on the model presented in Section II. The vehicle is assumed to operate near hover (non-acrobatic flight), hence the cross coupling terms are ignored in (9) and state derivatives $\dot{P}, \dot{Q}, \dot{R}$ are assumed to be proportional to the controller demands:

$$\begin{bmatrix} \dot{P} \\ \dot{Q} \\ \dot{R} \end{bmatrix} = \text{diag}\left(\frac{1}{I_x}, \frac{1}{I_y}, \frac{1}{I_z}\right) \begin{bmatrix} U_2 \\ U_3 \\ U_4 \end{bmatrix} \tag{20}$$

Similar approximations are made to (10) and (11) to obtain

$$\dot{z} = W \tag{21}$$
$$\dot{\phi} = P \tag{22}$$
$$\dot{\theta} = Q \tag{23}$$
$$\dot{\psi} = R \tag{24}$$

The total thrust is calculated in the Earth-fixed frame meaning the thrust from the rotors F_{pz} must be multiplied by the appropriate factors in the S_b matrix (2). Using (3) and (7) the total thrust demand is known. Based on these approximations, a PD scheme is used for the controller block, K, with the individual commands:

$$U_1 = -\frac{m}{c\phi c\theta}(K_{pz}(z_d - z) - K_{dz}(\dot{z}) + g) \tag{25}$$
$$U_2 = (K_{p\phi}(\phi_d - \phi) - K_{d\phi}(\dot{\phi})) \tag{26}$$
$$U_3 = (K_{p\theta}(\theta_d - \theta) - K_{d\theta}(\dot{\theta})) \tag{27}$$
$$U_4 = (K_{p\psi}(\psi_d - \psi) - K_{d\psi}(\dot{\psi})) \tag{28}$$

The gain values were tuned by trial and error and are identical for the roll and pitch controllers (26) and (27) since the vehicle has planes of symmetry along the x and y body axes and so it is possible to equate the pitch and roll responses to a rotor thrust. The gain values for the yaw controller, (28), are set lower than for the roll and pitch since the gyroscopic drag generated by the rotor turning is lower than the moment created when a rotor speed is increased. This means that the yaw response is more sluggish than the roll and pitch response.

IV. Rotor Saturation and Linear Control Allocation

A. Rotor Saturation

The allowable values of the rotor speeds $\Omega_i(t)$ are limited between absolute lower and upper bounds $\underline{\Omega}_i$, $\overline{\Omega}_i$ such that

$$\underline{\Omega}_i \leq \Omega_i(t) \leq \overline{\Omega}_i \tag{29}$$

holds for all t. There is a maximum thrust that can be generated by each motor-propeller combination due to the constraint on the maximum rotational speed, as well as a minimum thrust due to the lowest rotation speed of the rotor. Furthermore, it is assumed that the motors cannot turn backwards so a negative thrust cannot be generated. Hence, for the octorotor, $\underline{\Omega}_i \geq 0$. Test bed modeling can reveal the limit to the rate at which the motors can respond but in this paper no motor dynamics are modeled and it is assumed that the rotors respond instantaneously. Hence no constraint on the control rates is imposed. From (18), (29) can be rewritten as

$$\underline{\Sigma}_i \leq \Sigma_i(t) \leq \overline{\Sigma}_i \tag{30}$$

Repeating (17), the mapping of the generation of moments to the thrusts from the rotors is

$$\Gamma = \Lambda\Sigma \tag{31}$$

where for the octorotor, with all rotors operational, the dimension of Λ is 4×8 and the full control allocation matrix is given by (19). It should be noted that this differs from the control mapping of a quadrotor where the dimension of Λ is 4×4 [27] and a simple matrix inversion is used to determine the individual rotor thrust values based on the control demands.

For the octorotor a pseudo-inverse method is used. Ideally the thrust demands are shared between all eight rotors. This ensures that no single rotor is close to its maximum threshold which for these simulations was set at 700 rad/s. If an unattainable command is demanded by the controller then the allocation block will not pass it forward to the dynamics block. This is achieved using the redistributed pseudo inverse (RPI) method which is outlined in Section IV-B. This method allows for a control reallocation following a rotor failure. The dimension of the matrix Λ is reduced to $4 \times (8 - q)$ where q is the number of failed rotors. The outputs of the individual rotors are then capable of providing the required thrust until their maximum is reached. At this point they are saturated and no more thrust can be generated. In such a state the vehicle may not be controllable.

B. Redistributed Pseudo Inverse (RPI) Method

The redistributed pseudo inverse method extends the pseudo inverse method by explicitly accounting for actuator saturations. The method is originally attributable to [21], the method we use here is based on the description in [14]. A similar approach, called the Cascaded Generalized Inverse method is proposed by [28]. The process is iterative in that a succession of pseudo inverse solutions are calculated with position saturated control effectors removed from subsequent pseudo inverse solutions. The algorithm is

Step 1. Set $\tilde{\Lambda} = \Lambda$ and $c_i = 0$ for all i.

Step 2. Solve the modified pseudo inverse control allocation problem:

$$\Sigma = -c + \tilde{\Lambda}^{+}[\Gamma + \Lambda c] \tag{32}$$

where $\cdot^{+}$ denotes the Moore-Penrose pseudo inverse.

Step 3. If $\underline{\Sigma}_i < \Sigma_i < \overline{\Sigma}_i$ for all i, then end. Otherwise,

- for all i such that $\Sigma_i \leq \underline{\Sigma}_i$, set $c_i = -\underline{\Sigma}_i$ and remove the ith column of $\tilde{\Lambda}$ and
- for all i such that $\Sigma_i \geq \overline{\Sigma}_i$, set $c_i = -\overline{\Sigma}_i$ and remove the ith column of $\tilde{\Lambda}$

and return to Step 2.

The scheme is simply adapted for a control reallocation scheme in the event of an actuator failure by augmenting Step 1. Following a total failure in the jth actuator, remove the jth column of $\tilde{\Lambda}$ and remove c_j. Then proceed as above.

V. SIMULATIONS

In order to test the performance of the redistributed pseudo inverse reallocation method combined with the PD controller, simulations of a number of scenarios were carried out using MATLAB/Simulink. All scenarios began with the vehicle in a hover with all of the state derivatives equal to zero, and the aim is to maintain hover despite multiple rotor failures. The failure condition was initiated at a time of $t = 3$s via a switch in the simulation. It is assumed that the time taken for rotor fault detection and controller reallocation is 0.5s.

Four scenarios were investigated:

1) Failure in rotor 7.
2) Failure in rotor 0 and 7.
3) Failure in rotor 1, 5 and 7.
4) Failure in rotor 1, 3, 5 and 7.

The flight path of the vehicle is described by its altitude (z) and three Euler angles (ϕ, θ, ψ). After the failure the vehicle should recover level flight and regain any lost altitude.

A. Altitude Recovery

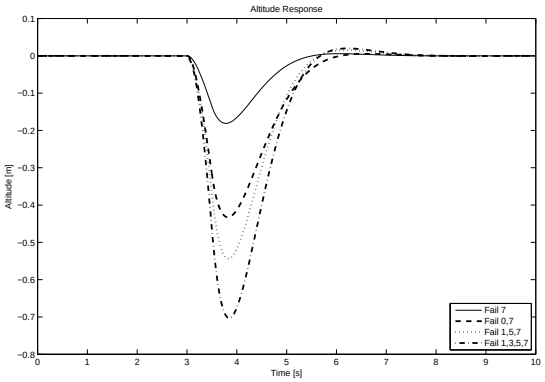

Fig. 3. Altitude Response

Figure 3 shows that as the number of failed rotors increases the altitude drop increases. This is as expected since the total thrust available drops. The vehicle recovers after the reconfiguration to regain the initial altitude with a similar performance after all rotor failures.

B. Roll Recovery

Figure 4 shows that failure in the rotor caused the vehicle to roll towards the failed rotors. The largest variation from level attitude was with two failed rotors that were next to each other. This generated a large adverse rolling moment before the vehicle recovered to level hover. When four rotors failed, because of the symmetry, no adverse rolling moment was generated and the failed-rotor vehicle acted like a quadrotor with only altitude disturbance.

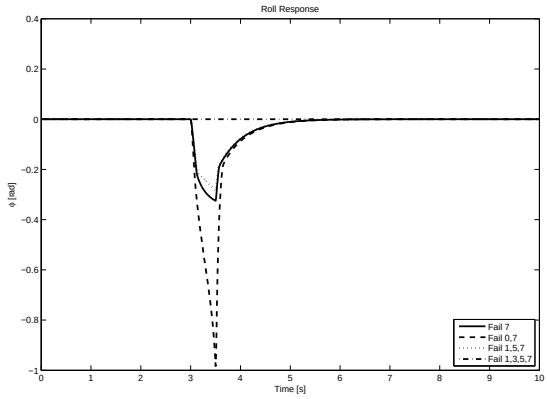

Fig. 4. Roll Response

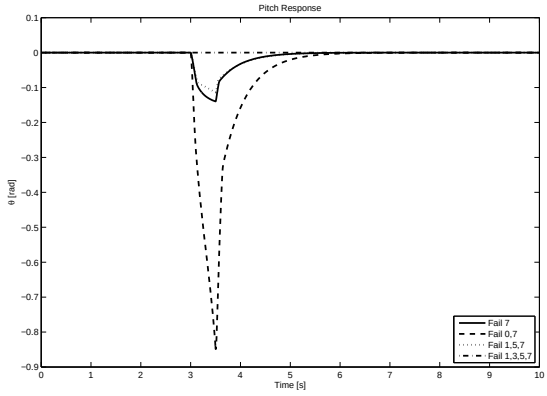

Fig. 5. Pitch Response

C. Pitch Recovery

Figure 5 shows that the pitch responses are similar to the roll response due to the symmetry over the x and y body axes. The differences in response after the failures were due to the physical location of the failed rotors. The response after reconfiguration is similar to the roll recovery and the vehicle regains hover. Again, with four rotor failures the vehicle only deviates in altitude.

D. Yaw Recovery

Figure 6 shows that the yaw moment generated from a failed rotor caused the vehicle to yaw slightly. But due to the highly coupled nature of the octorotor dynamics (9) the roll and pitch lead to a large adverse yaw disturbance.

The large roll and pitch generated with a failure in rotors 0 and 7 leads to a large divergence in yaw. The response of the vehicle once reconfigured is not the same as the roll and pitch responses due to the different gains chosen for this controller as described in Section III

VI. CONCLUSION

The paper proposes the use of a redistributed pseudo inverse method of control reallocation for the fault tolerant control of

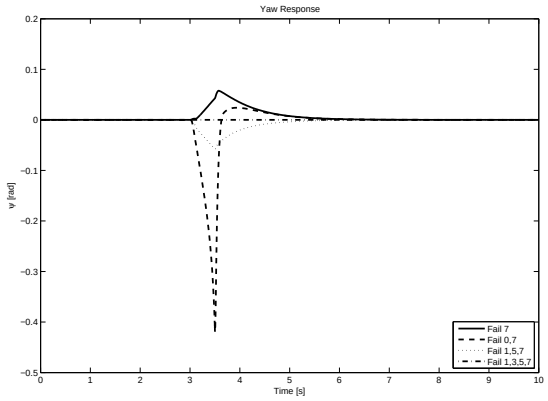

Fig. 6. Yaw Response

an octorotor VTOL aircraft. Unlike the quadrotor, the vehicle stability and performance is resilient to single rotor failure. Furthermore multiple rotor failures can be tolerated; control can be maintained for up to four rotor failures. Four scenarios were investigated by simulation and in all of them the vehicle retained enough control authority to recover from upset angles up to $60°$. Note that the proposed method depends on the availability of a fault detection system, this aspect has not been addressed in this paper.

Ongoing theoretical work is investigating the effect of redistributing the rotors so they turn clockwise, counter-clockwise alternating around the vehicle and finding an optimum configuration which will maximize the resilience of the system to multiple rotor failure. In future work, the method will be flight tested.

REFERENCES

[1] B. Michini, J. Redding, N. Ure, M. Cutler, and J. How, "Design and flight testing of an autonomous variable-pitch quadrotor," in *2011 IEEE International Conference on Robotics and Automation (ICRA)*, Shanghai, China, May 2011, pp. 2978 –2979.

[2] S. Bouabdallah, A. Noth, and R. Siegwart, "PID vs LQ control techniques applied to an indoor micro quadrotor," in *Proceedings EEE/RSJ International Conference on Intelligent Robots and Systems (IROS 2004).*, vol. 3, Sendai, Japan, Sep. 2004, pp. 2451 – 2456.

[3] S. Waslander, G. Hoffmann, J. S. Jang, and C. Tomlin, "Multi-agent quadrotor testbed control design: integral sliding mode vs. reinforcement learning," in *Proceedings 2005 IEEE/RSJ International Conference on Intelligent Robots and Systems (IROS 2005)*, Edmonton, Canada, Aug. 2005, pp. 3712 – 3717.

[4] Q.-L. Zhou, Y. Zhang, C.-A. Rabbath, and D. Theilliol, "Design of feedback linearization control and reconfigurable control allocation with application to a quadrotor UAV," in *Conference on Control and Fault-Tolerant Systems (SysTol)*, Oct. 2010, pp. 371 –376.

[5] S. Salazar-Cruz and R. Lozano, "Stabilization and nonlinear control for a novel trirotor mini-aircraft," in *Proceedings of the 2005 IEEE International Conference on Robotics and Automation (ICRA 2005)*, Barcelona, Spain, Apr. 2005, pp. 2612 – 2617.

[6] M. Ranjbaran and K. Khorasani, "Fault recovery of an under-actuated quadrotor aerial vehicle," in *49th IEEE Conference on Decision and Control (CDC)*, Dec. 2010, pp. 4385 –4392.

[7] F. Sharifi, M. Mirzaei, B. Gordon, and Y. Zhang, "Fault tolerant control of a quadrotor uav using sliding mode control," in *2010 Conference on Control and Fault-Tolerant Systems (SysTol)*, Oct. 2010, pp. 239 –244.

[8] Y. Zhang and A. Chamseddine, *Automatic Flight Control Systems - Latest Developments*. InTech, 2012, ch. 5. Fault Tolerant Flight Control Techniques with Application to a Quadrotor UAV Testbed.

[9] C. Berbra, S. Lesecq, and J. Martinez, "A multi-observer switching strategy for fault-tolerant control of a quadrotor helicopter," in *16th Mediterranean Conference on Control and Automation*, Ajaccio-Corsica, France, Jun. 2008, pp. 1094 –1099.

[10] A. Freddi, S. Longhi, and A. Monteriù, "A model-based fault diagnosis system for a mini-quadrotor," in *7th workshop on Advanced Control and Diagnosis*, Zielona Góra, Poland, Nov. 2009, pp. 2055 –2060.

[11] A. Freddi, A. Lanzon, and S. Longhi, "A feedback linearization approach to fault tolerance in quadrotor vehicles," in *Proceedings of the 18th IFAC World Congress*, Milano, Italy, Sep. 2011, pp. 5413 – 5418.

[12] T. Matsuzaki, I. Yamamoto, N. Inagawa, T. Nakamura, W. Batty, and J. F. Whidborne, "Development of unmanned flying observation robot with real time video transmission system," in *Proc. World Automation Congress (WAC 2010)*, Kobe, Japan, Sep. 2010, p. 5 pages, article number 5665710.

[13] V. G. Adîr, A. M. Stoica, A. Marks, and J. F. Whidborne, "Modelling, stabilization and single motor failure recovery of a 4Y octorotor," in *Proc. 13th IASTED International Conference on Intelligent Systems and Control (ISC 2011)*, Cambridge, U.K., Jul. 2011, pp. 82–87.

[14] M. W. Oppenheimer, D. B. Doman, and M. A. Bolender, "Control allocation for over-actuated systems," in *Proc. 14th Mediterranean Conference on Control and Automation (MED 06.)*, Ancona, Italy, Jun. 2006, paper no. FEA4-3.

[15] G. J. Ducard, *Fault-tolerant Flight Control and Guidance Systems – Practical Methods for Small Unmanned Aerial Vehicles*, ser. Advances in Industrial Control. Springer London, 2009. [Online]. Available: http://dx.doi.org/10.1007/978-1-84882-561-1_5

[16] J. Berg, K. Hammett, C. Schwartz, and S. Banda, "An analysis of the destabilizing effect of daisy chained rate-limited actuators," *IEEE Transactions on Control Systems Technology*, vol. 4, no. 2, pp. 171 – 176, Mar. 1996.

[17] M. Bodson, "Evaluation of optimization methods for control allocation," *J. Guid. Control Dyn.*, vol. 25, pp. 703–711, 2002.

[18] M. Bodson and W. Pohlchuk, "Command limiting in reconfigurable flight control," *J. Guid. Control Dyn.*, vol. 21, pp. 639–646, 1998.

[19] D. Enns, "Control allocation approaches," in *Proc AIAA Guid., Nav. and Control Conf.*, Boston, MA, 1998, pp. 98–108.

[20] J. J. Burken, P. Lu, Z. L. Wu, and C. Bahm, "Two reconfigurable flight-control design methods: Robust servomechanism and control allocation," *J. Guid. Control Dyn.*, vol. 24, pp. 482–493, 2001.

[21] J. Virnig and D. Bodden, "Multivariable control allocation and control law conditioning when control effectors limit," in *Proc. AIAA Guid., Nav. and Control Conf.*, Scottsdale, AZ, Aug. 1994, pp. 572–582.

[22] O. Harkegard, "Dynamic control allocation using constrained quadratic programming," *J. Guid. Control Dyn.*, vol. 27, pp. 1028–1034, 2004.

[23] J. Ma, P. Li, W. Li, and Z. Zheng, "Performance comparison of control allocation for aircraft with control effectiveness uncertainties," in *Proc. Asia Simulation Conference - 7th International Conference on System Simulation and Scientific Computing (ICSC 2008)*, Beijing, P.R. China, Oct. 2008, pp. 164–169.

[24] S. Bouabdallah, P. Murrieri, and R. Siegwart, "Design and control of an indoor micro quadrotor," in *Robotics and Automation, 2004. Proceedings. ICRA '04. 2004 IEEE International Conference on*, vol. 5, May 2004, pp. 4393 – 4398.

[25] A. Mian and W. Daobo, "Nonlinear flight control strategy for an underactuated quadrotor aerial robot," in *IEEE International Conference on Networking, Sensing and Control (ICNSC 2008)*, Apr. 2008, pp. 938 –942.

[26] Y. Yu, C. Jiang, and H. Wu, "Backstepping control of each channel for a quadrotor aerial robot," in *International Conference on Computer, Mechatronics, Control and Electronic Engineering (CMCE)*, vol. 3, Aug. 2010, pp. 403 –407.

[27] S. Bouabdallah and R. Siegwart, "Backstepping and sliding-mode techniques applied to an indoor micro quadrotor," in *Proceedings IEEE International Conference on Robotics and Automation (ICRA 2005)*, Apr. 2005, pp. 2247 – 2252.

[28] K. A. Bordignon, "Constrained control allocation for systems with redundant control effectors," Ph.D. dissertation, Virginia Polytechnic Institute, VA, 1996.